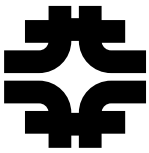

Fermi National Accelerator Laboratory

FERMILAB-Conf-98/097-E
CDF and D0

Top Quark Physics at the Tevatron

Pushpalatha C. Bhat
For the CDF and D0 Collaborations

Fermi National Accelerator Laboratory
P.O. Box 500, Batavia, Illinois 60510

April 1998

To be Published in the Proceedings of the *8th Lomonosov Conference on Elementary Particle Physics*, Moscow, Russia, August 25-29, 1997

Disclaimer

Distribution

FERMILAB-conf-98/097-E

Top Quark Physics at the Tevatron *

Pushpalatha C. Bhat
Fermi National Accelerator Laboratory, Batavia, IL 60510, USA
(for the CDF and DØ Collaborations)
(December 1997)

Abstract

We review the analyses of $t\bar{t}$ candidate events in various decay channels, carried out using the $p\bar{p}$ collider data at $\sqrt{s} = 1.8$ TeV by the CDF and DØ collaborations at the Fermilab Tevatron. The measurements of the top quark mass (m_t) using *lepton+jets* channel yield m_t=173.3±7.8 GeV/c^2 from DØ analysis and m_t=175.9±6.9 GeV/c^2 from CDF analysis. The production cross section is measured to be $\sigma_{t\bar{t}} = 7.6^{+1.8}_{-1.5}$ pb by CDF and $\sigma_{t\bar{t}} = 5.6 \pm 1.8$ pb by DØ. Further investigations using $t\bar{t}$ decays and future prospects are briefly discussed.

1. Introduction

The discovery of the top quark is a major triumph of the Standard Model and possibly the beginning of a new era in particle physics. Nearly two decades of intense research at various accelerator facilities around the world and remarkable efforts at the Tevatron over the last decade culminated in the observation [1,2] of the top quark, the heaviest fundamental particle thus far known. Since the first observation reported by the CDF and DØ collaborations in 1995, more than twice the data have been collected by each experiment (≥ 110 pb^{-1}), particle identification techniques have been refined, innovative analysis methods have been adopted and impressively

*Plenary talk presented at the VIII Lomonosov Conference on Elementary Particle Physics, Aug 25-29, 1997, Moscow, Russia.

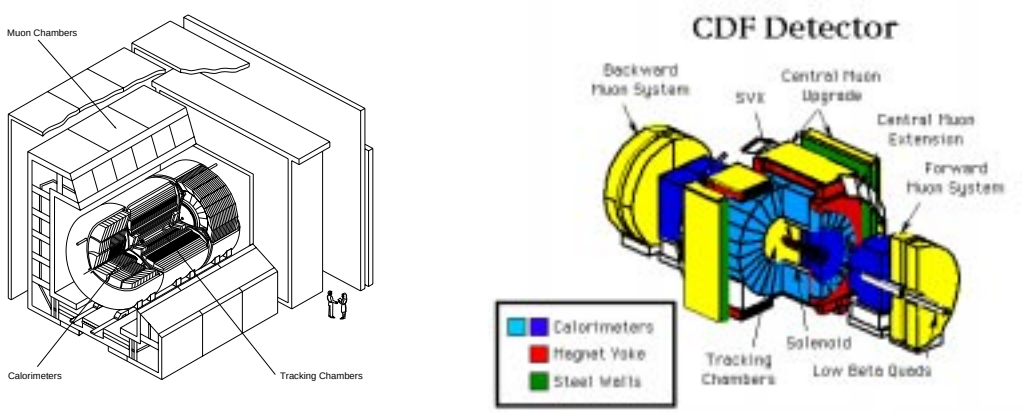

FIG. 1. Schematic views of the DØ detector (left) and the CDF detector (right).

precise measurements of the mass of the top quark and the $t\bar{t}$ production cross section have been made. In this review, we describe these studies and the current status of top quark physics. We report the updated results available at the time of this writing.

2. The CDF and DØ Detectors

The CDF [3] and DØ [4] detectors at Fermilab are both designed to provide efficient identification and excellent measurements of electrons, muons and jets. The schematic views of both detectors are shown in Fig. 1.

The CDF detector has a four-layer silicon vertex detector (SVX) located immediately outside the beam pipe, vertex time projection chambers (VTX) and the central tracking chamber (CTC) inside a 1.4T solenoidal magnet. The SVX provides precise track reconstruction in the plane transverse to the beam and is used to identify secondary vertices from b- and c-quark decays. The track impact parameter resolution is $\approx (13 + 40/p_T)\mu$m, where p_T is the transverse momentum of the track. The central electromagnetic (CEM) and hadronic calorimeters (CHA) ($|\eta| < 1.1$) employ a projective tower geometry ($\Delta\eta \times \delta\phi \approx 0.1 \times 15^\circ$), and are composed of scintillators layered with lead and steel absorbers. A layer of proportional wire chambers is located at the shower maximum in the CEM. The plug and forward calorimeters ($1.1 < |\eta| < 4.2$) consist of gas proportional chambers as active media and lead and iron as absorber materials. They aid in electron and jet identification in $|\eta| < 4.2$. The energy resolution of the CDF central

calorimeter is $\frac{13.5\%}{\sqrt{E_T}} \oplus 2\%$ for EM showers and $\frac{50\%}{\sqrt{E_T}} \oplus 3\%$ for hadrons. The central muon (proportional drift) chambers have 80% geometrical coverage for $|\eta| < 0.6$, and the coverage is extended up to $|\eta| \simeq 1.1$ by the extension chambers.

The DØ detector comprises a central tracking system, a uranium/liquid-argon calorimeter and a muon spectrometer. The central tracking system provides charged particle tracking for $|\eta| < 3.2$ and consists of four sub-detector systems: a three-layer vertex drift chamber, a transition radiation detector(TRD), a four-layer central drift chamber and two forward drift chambers. A central and two end uranium/liquid-argon sampling calorimeters provide hermetic coverage ($|\eta| < 4.2$). Each of the calorimeters consist of electromagnetic, fine hadronic and coarse hadronic sections with a total of eight longitudinal depth segments and fine transverse segmentation of $\Delta\eta \times \Delta\phi = 0.1 \times 0.1$ (0.05×0.05 in the third EM layer, at EM shower maximum). The resolution of the calorimeter is measured to be $\frac{\sigma_E}{E} = \frac{15\%}{\sqrt{E}} \oplus 0.4\%$ for EM showers and $\frac{\sigma_E}{E} = \frac{50\%}{\sqrt{E}}$ for hadrons. The muon system ($|\eta| < 3.3$), made up of layers of proportional drift chambers and solid-iron toroidal magnets, is used to identify muons and measure their momenta with a resolution of $\sigma(1/p) = 0.18(p-2)/p^2 \oplus 0.008$ (with p in GeV/c).

The particle identification procedures adopted by the experiments are described in ref. [5,6]. The jets are reconstructed in both experiments using cone algorithm with $R = \sqrt{\Delta\eta^2 + \Delta\phi^2}$, where η is the pseudorapidity. CDF reconstructs jets with $R = 0.4$, while DØ generally uses jets reconstructed with cone $R = 0.5$ in the analyses described here. Both experiments correct the measured jet energies for detector response, contributions due to the underlying event, multiple interactions, and losses due to leakage out of the jet cone. DØ selects candidate events after applying these standard jet energy corrections while CDF applies the corrections after the initial selection, as needed.

3. Top Quark Production and Decays

In $p\bar{p}$ collisions at the Tevatron ($\sqrt{s} = 1.8$ TeV), top quarks are predominantly pair produced by $q\bar{q}$ annihilation ($\approx 90\%$) or gg fusion ($\approx 10\%$). The rate of single top quark production *via* the creation of a virtual W boson or *via* W-gluon fusion are calculated [7] to be much smaller. The $t\bar{t}$ production cross section has been calculated in perturbative QCD to next-to-leading order (NLO) and beyond, using resummation techniques [8], as a function of top mass. For m_t=175 GeV/c^2, the theoretical cross section

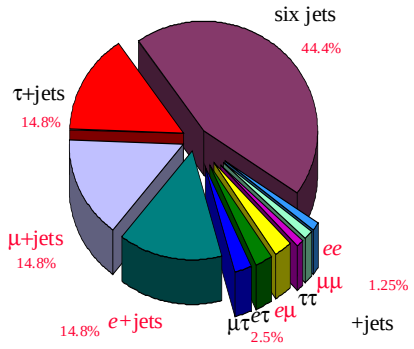

FIG. 2. Standard decay modes of $t\bar{t}$ events and their branching fractions.

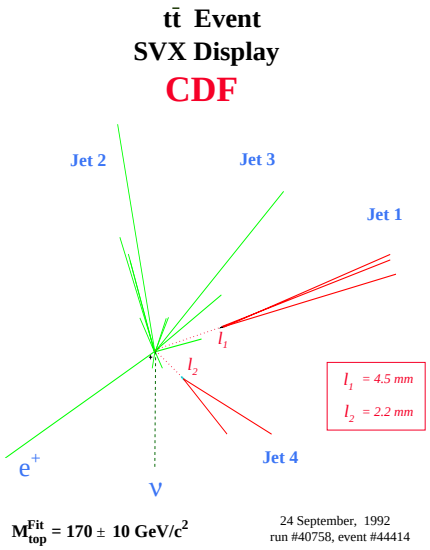

FIG. 3. A $t\bar{t} \to e$+jets candidate event from the CDF experiment. Jet 1 and Jet 4 are identified as b-quark decays by the SVX detector.

is in the range of 4.75 pb to 5.5 pb, about ten orders of magnitude lower than the total inelastic cross section at $\sqrt{s} = 1.8$ TeV. About 500 $t\bar{t}$ pairs are expected to have been produced in the 5×10^{12} or so $p\bar{p}$ collisions that occured at the CDF and DØ interaction regions during Run 1.

Since the top quark is very heavy, it decays before it has time to hadronize. The signatures for top production therefore come from decay modes of the top and anti-top quarks. According to the standard model, each top quark decays into a W boson and a b-quark. The $t\bar{t}$ events are categorized into *dilepton*, *lepton+jets* or *all-jets* channels depending on whether one or both of the W bosons decay leptonically or hadronically. The decay modes and the branching fractions are shown in Fig. 2. As an example of an event topology, a $t\bar{t} \to (W^+b)(W^-\bar{b}) \to (e^+\nu b)(q\bar{q}\bar{b})$ candidate event from the CDF experiment is shown in Fig. 3.

4. Measurements of the $t\bar{t}$ Production Cross Section

The analyses in various decay channels and the $t\bar{t}$ cross section measurements from Run I data are described here. Several papers by the CDF and DØ collaborations on these analyses have been either recently published or are soon to be published [9,10].

4.1 The Dilepton Channels

The signature for $t\bar{t}$ decay in these channels is the presence of two high-transverse energy (E_T), central, isolated leptons, two jets initiated by the b-quarks and a large missing transverse energy $\not\!\!E_T$ arising from the two neutrinos. The dominant backgrounds are from leptonic decays of the Z, the Drell-Yan process, vector boson pair production and QCD ($b\bar{b}$ and $c\bar{c}$). The ee and $e\mu$ channels have a small amount of background from events with fake electrons due to mis-identification of jets as electrons. The kinematic event selection criteria applied by DØ are shown in Table I. Additional cuts have been applied to ee and $\mu\mu$ channels to suppress the large background from leptonic Z decays. In the ee channel, if $|M_{ee} - M_Z| < 12\ GeV/c^2$, then the missing transverse energy measured in the calorimeter, $\not\!\!E_T^{cal}$, is required to be greater than 40 GeV. In the $\mu\mu$ channel, a kinematic fit to the Z has been performed and the event is required to be inconsistent with the Z +jets hypothesis ($P(\chi^2_{Zfit})$ be <1%). The other notable kinematic quantity is H_T (shown in Fig. 4) which is the scalar sum of E_T of the selected objects in the event. Three $e\mu$ events, one ee event and one $\mu\mu$ event remain as

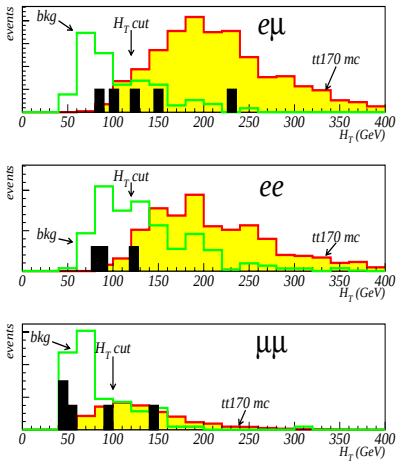

FIG. 4. The distributions of H_T for *dilepton* events (m_t=170 GeV/c^2 signal MC) from the DØ analyses. The location of data events are shown by dark histograms.

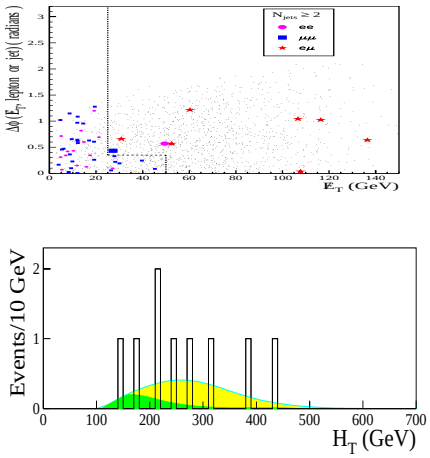

FIG. 5. (CDF) $\Delta\phi(\not\!\!E_T, \ell$ or $j)$ *vs.* $\not\!\!E_T$ (top); small dots show the signal. H_T distribution (bottom) for *dilepton* candidates, signal (lightly shaded area) and background (heavily shaded).

candidates. The backgrounds are estimated using MC simulations, and corrected for efficiencies measured in the data.

The more inclusive "$e\nu$" channel (studied by DØ to gain further signal acceptance) contains $t\bar{t}$ signal events mainly from *dilepton* channels and e+jets channel which fail the standard kinematic selection. Four eν events survive the selection criteria. The dominant background process for this channel is W($\rightarrow e\nu$)+jets production which is largely eliminated by the large $e\nu$ transverse mass requirement. The background is estimated using the number of W+ $\geq$2 jets events observed in the data before the cut on $M_T^{e\nu}$ and applying the efficiency of the cut as determined by MC.

The signal efficiencies for all *dilepton* channels are computed using HERWIG MC and GEANT-based detector simulation. The results are shown in Table II.

In the CDF analyses of the standard *dilepton* modes (ee, $e\mu$, $\mu\mu$), the following initial kinematic requirements are used: two oppositely charged leptons with $p_T > 20$ GeV/c within $|\eta| < 1.0$ (at least one isolated); $|M_{ee} - M_Z| > 15$ GeV/c^2; 2 jets with $E_T > 10$ GeV within $|\eta| < 2.0$; $\not\!\!E_T > 25$ GeV. If there is a photon in the event with $E_T > 10$ GeV, then the event is removed if it is consistent with radiative Z decay. To ensure that $\not\!\!E_T$ is not due to mismeasurements of the energies of leptons or jets, $\not\!\!E_T > 50$ GeV is required if the azimuthal angle between the direction of the $\not\!\!E_T$ vector and the nearest lepton or jet, $\Delta\phi(\not\!\!E_T, \ell \; or \; j)$ is less than 20^o (see Fig. 5). The H_T distributions of the candidate events, signal and background are also compared in Fig. 5. Nine events – seven $e\mu$, one ee and one $\mu\mu$ – survive the cuts.

CDF has also analyzed the "τ *dilepton*" channels, eτ and $\mu\tau$, where τ decays hadronically. The signal acceptance is estimated to be $(0.085 \pm 0.010(stat) + 0.012(syst))\%$ for the track-based selection that uses one-prong decays and $(0.134 \pm 0.013(stat) \pm 0.019(syst))\%$ for calorimeter-based analysis that uses one- and three-prong decays. Four events are seen in data, while ~ 2 background events and ~ 1 $t\bar{t}$ event are expected.

4.2 The Lepton+jets Channels

The characteristics of the signal in the *lepton+jets* channel are the presence of a high p_T, central, isolated lepton, with $\not\!\!E_T$ due to the neutrino and, several jets (two jets from the W decay and two from the b quarks). The final states studied contain single e/μ with three or more jets. The b-quarks in $t\bar{t}$ events are identified either by the b-decay vertices (CDF) [5]

	Dilepton	ℓ +jets	ℓ +jets/μ	eν
lepton p_T	> 15	> 20	> 20	> 20
	> 20 (ee)			
electron $\|\eta\|$	< 2.5	< 2.0	< 2.0	< 1.1
muon $\|\eta\|$	< 1.7	< 1.7	< 1.7	—
$\not\!\!E_T$	> 20 (eμ)	$> 25(e)$	> 20	> 50
	$> 25(ee)$	> 20 (μ)		
jet E_T	> 20	> 15	> 20	> 30
jet $\|\eta\|$	< 2.5	< 2.0	< 2.0	< 2.0
# of jets	≥ 2	≥ 4	≥ 3	≥ 2
H_T^e	> 120(ee,eμ)	–	–	–
H_T	$> 100(\mu\mu)$	> 180	> 110	–
$\mathcal{A}$	–	> 0.065	> 0.040	–
E_T^L	–	> 60	–	–
η_W	–	< 2.0	–	–
tag muon	–	veto	$p_T > 4$	–
			$\Delta\mathcal{R}_{jet} < 0.5$	
$M_T^{e\nu}$	–	–	–	> 115

TABLE I. Kinematic event selection criteria for various $t\bar{t}$ decay channels applied in the cross section analysis by DØ. All energies are in GeV; η is the pseudorapidity; $H_T = \sum E_T^{jet}$ with E_T^{jet} >15 GeV and $H_T^e = H_T + E_T^e$.

or by the semileptonic decays (CDF and DØ) of the b- or c-quarks (from b cascade decay). The dominant backgrounds are W+jets production with the W decaying to eν or $\mu\nu$ and, QCD multijet events with fake leptons and mismeasured $\not\!\!E_T$. Requiring one or more b-tags significantly improves the signal to background ratio in these channels. In the absence of a b-tag in the event, event shape and kinematic characteristics can be employed to enhance the signal to background ratio, as is done by DØ in the so-called "topological analysis".

The three powerful discriminants used in the DØ topological analysis are: H_T which is the sum E_T of all the selected jets, aplanarity $\mathcal{A}$ calculated as $\frac{2}{3}$ × smallest eigenvalue of the total normalized momentum tensor in the event and, the total leptonic E_T, $E_T^L = E_T^{e/\mu} + \not\!\!E_T$. Requiring large E_T^L suppresses the background from fakes. Large H_T signifies the decay of

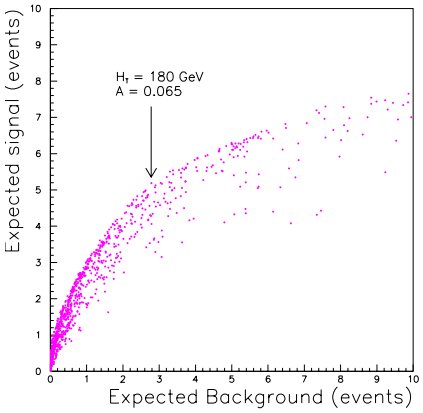

FIG. 6. (DØ) Expected signal (180 GeV/c^2 top) versus background yields in 77 pb^{-1} for various cuts on $\mathcal{A}$ and H_T, in the *e+jets* channel, as found by the *Random Grid Search* Method.

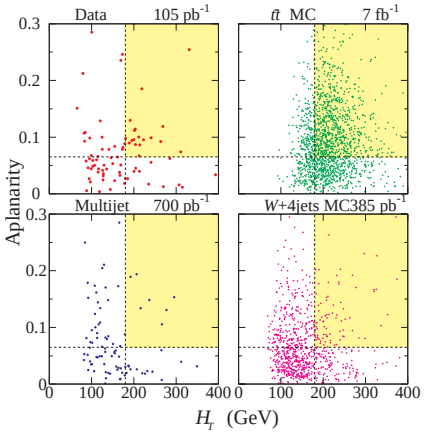

FIG. 7. (DØ) Distributions in ($\mathcal{A}$, H_T) plane for data(top left), $t\bar{t}$ MC(top right), multijet background (bottom left) and W+jets VECBOS MC(bottom right).

massive objects. The aplanarity variable would have a value of half for spherical events and zero for planar events; $t\bar{t}$ events are expected to be more spherical than the radiative QCD processes and hence have larger values of aplanarity.

An optimum set of cuts for $\mathcal{A}$ and H_T has been deduced by performing a *random grid search* [13]. Each event in the signal Monte Carlo (180 GeV/c^2 $t\bar{t}$) is used to provide the possible sets of cuts in the ($\mathcal{A}$, H_T) space for the random grid search. The results are shown in Fig. 6. Each point on this plot corresponds to a possible set of conventional cuts, and the points on the outer envelope maximize the signal efficiency corresponding to given background estimates. The set of cuts that yields the smallest expected fractional error in cross section is chosen ($\mathcal{A} = 0.065$ and $H_T = 180$ GeV). The two dimensional distributions of ($\mathcal{A}$, H_T) for signal, background and data samples along with the cuts applied are displayed in Fig. 7. The W+jets background is modeled using VECBOS MC and the fake lepton background by multijet data. The selection cuts yield 19 events in the data ($\int \mathcal{L}dt \sim$110 pb^{-1}), and an expected background of 8.7 $\pm$ 1.7 events.

Since every $t\bar{t}$ event has two b-quarks, DØ expects ~20% of the events to have a *detectable* soft muon coming from the semi-leptonic decays of the b-quarks. In the background, however, only ~2% of the events are expected

to have a soft muon b-tag. In the b-tag analysis, the event shape cuts are relaxed and a minimum of only three jets are required in the event. The event selection cuts and b-tag requirement are shown in Table I. The number of observed events and estimated background as a function of jet multiplicity before $\mathcal{A}$ and H_T cuts are shown in Fig. 8. The jet multiplicity spectrum for background is obtained by convoluting the jet multiplicity spectrum for untagged events with the measured b-tag rate. The b-tag rate is determined from data and is observed to be a function of the jet E_T and the number of jets in the event. An excess of events with three or more jets can be clearly seen in Fig. 8. The optimal cuts for $\mathcal{A}$ and H_T are determined using the random grid search method. After the event shape cuts, 11 events are observed in the data while the total estimated background is 2.6 $\pm$ 0.6 events.

In the CDF analysis, only b-tagged (SVX or SLT) events are used. The initial sample is required to contain an isolated electron (muon) with E_T >20 GeV (p_T >20 GeV/c) within $|\eta|$ <1.0, $\geq$3 jets with E_T >15 GeV and $|\eta|$ <2.0, and $\not\!\!E_T$ >20 GeV. Events consistent with Z candidates and *dilepton* candidates are vetoed. The efficiency for SVX tagging at least one b-quark in a $t\bar{t}$ event with $\geq$ 3 jets is estimated to be (39 $\pm$ 3)% using $t\bar{t}$ MC and detector simulation studies. Efficiency for SLT b-tagging is (18 $\pm$

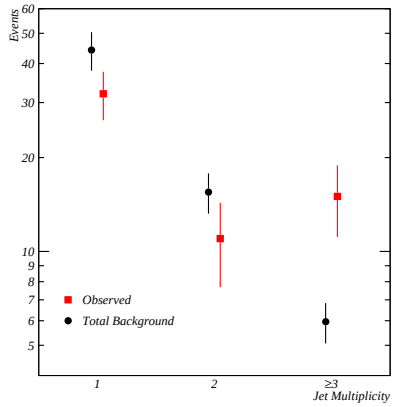

FIG. 8. Jet multiplicity of b-tagged *lepton+jets* events before Aplanarity and H_T cuts. Square points represent DØ data and the circles the expected background.

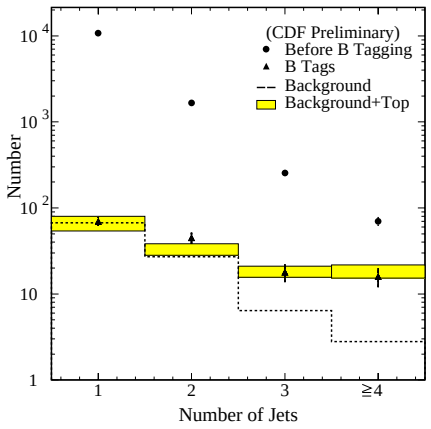

FIG. 9. Jet multiplicity of b-tagged *lepton+jets* events from CDF data. See legend on the plot for details.

Channel	$\epsilon \times BR(\%)$	Data	Background	$\sigma_{t\bar{t}}$(pb)
$\ell\ell$(with eν)	0.91 ± 0.17	9	2.6 ± 0.6	6.4±3.4
ℓ +jets(topol.)	2.27 ± 0.46	19	8.7 ± 1.7	4.1 ± 2.1
ℓ+jets/μ	0.96 ± 0.15	11	2.4 ± 0.5	8.3 ± 3.6
Combined	4.14 ± 0.69	39	13.7 ± 2.2	5.6 ± 1.8
All jets	1.8 ± 0.4	44	25.3 ± 3.1	7.9 ± 3.5

TABLE II. Summary of results from DØ cross section analyses. The top quark mass used for efficiency and cross section calculations is 172 GeV/c^2.

	Lepton+Jets		Dilepton*	All-Hadronic	
Tag	SVX	SLT	-	SVX	2 SVX
ϵ_{total}	0.037 ± 0.005	0.017 ± 0.0003	0.0074 ± 0.0008	0.044 ± 0.010	0.030 ± 0.010
Obs. Events	34	40	9	187	157
Background	9.2 ± 1.5	22.6 ± 2.8	2.4 ± 0.5	142 ± 12	120 ± 18
$\sigma_{t\bar{t}}(pb)$	$6.2^{+2.1}_{-1.7}$	$9.2^{+4.3}_{-3.6}$	$8.2^{+4.4}_{-3.4}$	$9.6^{+4.4}_{-3.6}$	$11.5^{+7.7}_{-7.0}$

TABLE III. Summary of acceptance factors and measured cross sections from CDF for each analysis channel. m_t=175 GeV/c^2 used. * Does not include $e\tau$ and $\mu\tau$ channels.

2)%. In $W+ \geq 3$ jets sample, 34 SVX-tagged events containing a total of 42 SVX tags and 40 SLT-tagged events containing a total of 44 SLT tags, remain. Of these, 11 events are b-tagged by both algorithms.

The dominant background from W+heavy-flavor production processes are estimated using HERWIG and VECBOS MC programs and b-tag efficiency estimated using data. The non-W background and the number of events with mis-tags are estimated using data. The background to SLT tagged events mainly arising from W$b\bar{b}$,W$c\bar{c}$, hadrons misidentified as leptons, decays in flight and other fake backgrounds are estimated using W+jets data and MC. Excess above background is clearly seen for $W+ \geq 3$ jets (see Fig. 9).

The signal acceptance in the *lepton+jets* channel for $t\bar{t}$ events with assumed m_t=175 GeV/c^2 is calculated using a combination of data, PYTHIA and HERWIG $t\bar{t}$ MC. A summary of event yields, signal eficiency, background estimates and measured cross section are shown in Table III.

4.3 The All-jets Channel

This multijet final state has the biggest share of the $t\bar{t}$ decays ($\approx 44\%$),

but is overwhelmed by QCD multijet background. To overcome this huge background, stringent kinematic cuts and b-tagging are employed.

The initial selection for the approaches used by CDF require five or more jets with $E_T > 15$ GeV, $|\eta| < 2.0$ and $H_T > 300$ GeV and at least one jet to be b-tagged. This results in 1596 events with $S/B \approx \frac{1}{20}$. Then, in the first approach, $H_T/\sqrt{\hat{s}} > 0.75$ is required ($\sqrt{\hat{s}} \equiv$ invariant mass of the multijet system). The aplanarity of the event is required to satisfy $\mathcal{A} > -0.0025 H_T^3 + 0.54$, where $H_T^3 = H_T - E_T^{jet1} - E_T^{jet2}$. (Such cuts in (A, H_T) plane were first used by DØ [15].) A total of 187 events are selected containing 222 b-tags. The number of b-tags expected from the background is $164.8 \pm 1.2 \pm 10.7$. The probability for the background to fluctuate to the observed number of b-tags or more is $\mathcal{P} = 1.5 \times 10^{-3}$, corresponding to a 3σ for a Gaussian distribution. Using the efficiency calculated with HERWIG MC, the cross section at $m_t = 175$ GeV/c^2 is measured as $\sigma_{t\bar{t}} = 9.6 \pm 2.9(\text{stat}) \pm^{3.3}_{2.1}(\text{sys})$ pb.

In the second approach, requiring ≥ 2 b-tags, 157 events are observed while the predicted background is 122.7 ± 13.4 events from QCD heavy flavor and fake double tags. The measured cross section from this analysis is $11.5 \pm 5.0(\text{stat})^{+5.9}_{-5.0}(\text{syst})$ pb. The probability for background fluctuating to the observed number of tags is $\mathcal{P} = 2.5 \times 10^{-2}$, corresponding to a 2σ effect for a Gaussian distribution. Combining the two analyses while taking into account the correlation of $(34 \pm 13)\%$ between them, $\sigma_{t\bar{t}} = 10.1 \pm 1.9(\text{stat})^{+4.1}_{-3.1}(\text{sys})$ pb is obtained for $m_t = 175$ GeV/c^2.

The DØ analysis requires six or more jets ($R = 0.3$ cone) with $E_T > 15$ GeV, $|\eta| < 2.0$. One of the jets is required to be b-tagged (soft lepton tag), in the final sample. A total of 13 kinematic and event shape parameters including H_T, H_T^3, $\sqrt{\hat{s}}$, E_T^{jet1}/H_T, aplanarity, sphericity, centrality, jet-width, p_T of the tag-μ and a mass likelihood parameter [14] are used in a neural network analysis (see Fig. 10). A cross section measurement of $\sigma_{t\bar{t}} = 7.9 \pm 3.1(\text{stat}) \pm 1.7(\text{sys})$ pb at $m_t = 172$ GeV/$c^2$is obtained by fitting the NN distribution for data to signal plus background contributions. In the signal region, defined with NN-output >0.79, 44 events are observed in data, the expected background being 25.3 ± 3.1 events. The significance of the excess is 3.2 standard deviations.

4.4 The $t\bar{t}$ Cross Section

The number of observed events, estimated background, signal efficiencies and the measured cross sections from analyses in the *dilepton*, *lepton+jets*

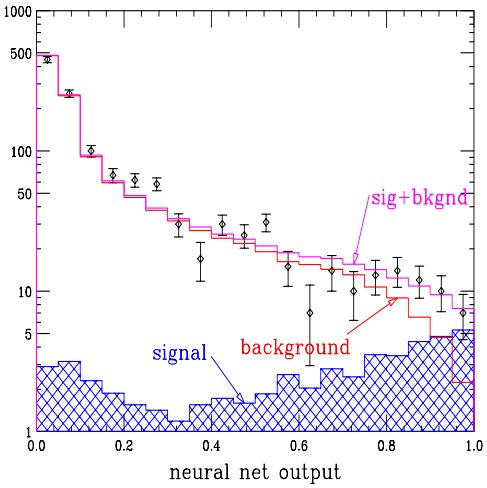

FIG. 10. (DØ) NN output distribution for data (points) fit to signal (hatched histogram) and background (dashed histogram).

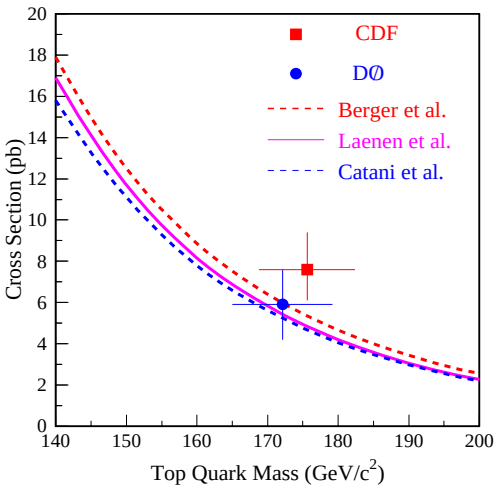

FIG. 11. $t\bar{t}$ production cross section measured by CDF and DØ, compared with the theoretical calculations.

and *all-jets* channels from DØ and CDF experiments are summarized in Tables II and III. The measurement from CDF with all channels combined (except $e\tau$ and $\mu\tau$), yields $\sigma_{t\bar{t}} = 7.6^{+1.8}_{-1.5}$ pb (at m_t=175 GeV/c^2). The combined measurement from DØ (all channels included except preliminary *all-jets* results) is $\sigma_{t\bar{t}}$=5.6 $\pm$1.8 pb assuming m_t=172 GeV/c^2. The $t\bar{t}$ cross sections measured by the two experiments are displayed along with theoretical calculations in Fig. 11.

5. Direct Measurement of the Top Quark Mass

A precision measurement of the top quark mass, along with that of the W boson, would provide constraints on the yet unobserved Higgs boson. The top quark mass, therefore, is one of the most important parameters in the Standard Model. Both collaborations have measured the top quark mass using events from various $t\bar{t}$ decay channels. The measurement with the smallest error for both experiments comes from the *lepton+jets* channel.

The standard procedure for measuring the top quark mass would be to perform a kinematic fit to constrain each candidate event to a $t\bar{t}$ decay hypothesis yielding an estimate of the best fit mass m_{fit} and a χ^2_{fit}, and, subsequently extract a maximum likelihood estimate of the top quark mass

(m_t) from the entire sample. In the absence of inital and final state gluon radiation, there are 6 decay particles in the final state of $t\overline{t}$ decay. Each particle is described by a 3-momentum, leading to a total of 18 observables. p_T of the hadronic system recoiling against $t\overline{t}$, adds two more variables. There are 5 kinematic constraints that can be applied to the fit–the masses of the top and antitop quarks are equal, the effective masses of the decay products of the two W bosons equal the W mass and the two transverse components of the recoil system equal those of the $t\overline{t}$ system. If all 20 observables are measured as in the case of the *all-jets* channel, then one has a 5C fit. For the *all-jets* channel, however, the measurement of the recoil system is ignored and a 3C fit is performed (CDF analysis). In the case of the *lepton+jets* channel, only two of the five constraints remain, since the 3-momentum of the neutrino is not measured. The kinematics of the *dilepton* events are underconstrained (-1C) since there are two unobserved neutrinos. One can, however, solve the $t\overline{t}$ system in the *dilepton* channel with zero constraints, assuming a top quark mass, and use the likelihood distribution for candidate events to obtain a maximum likelihood estimate of the top quark mass from the sample. This is the approach used by DØ.

It is also possible to extract the top quark mass using one or more observables that have strong dependence on the top quark mass. CDF adopts this method for the measurement of the top quark mass from the *dilepton* channels. The results presented here are published by the CDF and DØ collaborations recently [10,12].

5.1 DØ Lepton+jets Mass Analysis

A breakthrough in the DØ analysis comes from using multivariate methods [15] to compute signal probability p_{top} for each event and including this information along with m_{fit} for the event in a two dimensional likelihood fit analysis in the (m_{fit}, p_{top}) plane to extract the top quark mass.

The initial selection of events is similar to that used in the cross section analysis, except that at least four jets are required even in the presence of b-tags and no cuts on $\mathcal{A}$ and $\mathcal{H}_T$ are applied. 91 events are selected with the initial selection cuts, with 7 b-tagged events.

The $t\overline{t}$ signal events are simulated using HERWIG MC and W+jets background is modeled with VECBOS MC (HERWIG used for fragmenting partons to jets). The cross section normalization for W+jets production is inferred from data. The ≈20% of background events from non-W sources are modeled by multijet data.

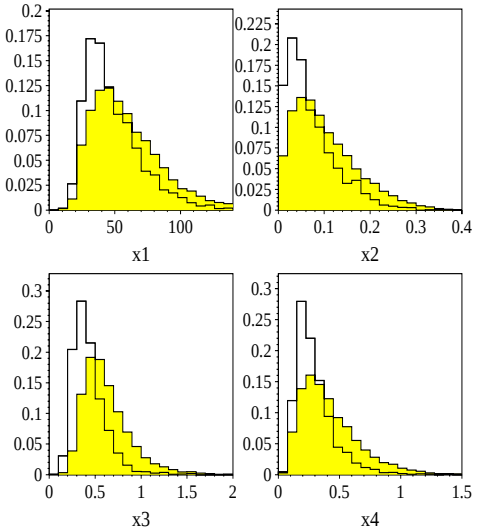

FIG. 12. (DØ) Distributions of the variables x1, x2, x3 and x4 (see text for definitions) for signal (shaded histograms) and for background (unshaded histograms).

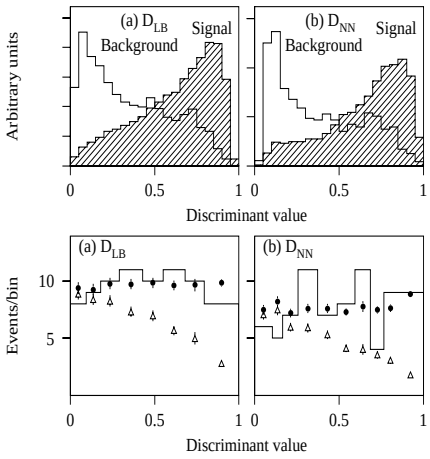

FIG. 13. (DØ) $\mathcal{D}_{\mathcal{LB}}$ and $\mathcal{D}_{\mathcal{NN}}$ for signal and background (top). The distributions for data (histograms) are compared to signal+background (circles) and background (triangles) (bottom plots).

Since the energy scale is crucial for a reliable mass measurement, more elaborate jet energy corrections are applied in this analysis. The standard corrections described in section 2 are applied before event selection. Each jet in the event (both for the data and MC) is then corrected to parton energy; the correction is different depending on whether the jet is assigned to a light quark or a b-quark. This, on average, better corrects for neutrinos from b decay, and sharpens the resolution in m_{fit}. Finally, an η-dependent correction derived from a study of γ+jet events in data and MC, is applied to the data and MC energy scales. Based on studies of E_T balance in γ+jets and Z+jets events, variations of cuts employed in these studies and modeling of the underlying event, a jet energy scale error of $\pm(2.5\%+0.5$ GeV) is assigned.

Two independent multivariate techniques are used to calculate boundaries between the signal and background classes of events in mulitdimensional space to obtain optimal separation [15]. After an extensive search for variables that provide good discrimination between signal and background and are weakly correlated with m_{fit}, the following variables are chosen:

- $x_1 \equiv \not\!\!E_T$
- $x_2 \equiv \mathcal{A}$, aplanarity of the event, defined earlier.
- $x_3 \equiv \frac{H_T - E_T^{jet1}}{H_z}$, where $H_T = \sum E_T$ of all selected jets, $H_z \equiv \sum |E_z|$ of all objects in the event (lepton, neutrino and the jets), E_z being the momentum component of the object in the beam direction. x_3 measures the centrality of the event.
- $x_4 \equiv \frac{\Delta R_{jj}^{min} \cdot E_T^{min}}{E_T^L}$, where ΔR_{jj}^{min} is the minimum ΔR of the six pairs of four jets and E_T^{min} is the smaller jet E_T from the minimum ΔR pair. The x_4 variable measures the extent to which the jets are clustered together.

On average, the signal events have larger values of the variables than background events (see fig. 12). These variables are combined into a single multivariate discriminant $\mathcal{D}(x) = \frac{s(x)}{s(x)+b(x)}$, where $s(x)$ and $b(x)$ are the signal and background densities. The two multivariate methods used are: (1) a log likelihood technique referred to as "low bias"(LB) method and (2) a feed-forward neural network (NN). In the LB method, the ratios $L_i(x_i) = \frac{s_i(x_i)}{b_i(x_i)}$ are parametrized in each variable integrating over others. Then $\ell nL = \sum_i w_i \ell n L_i$ are formed where the weights w_i are adjusted

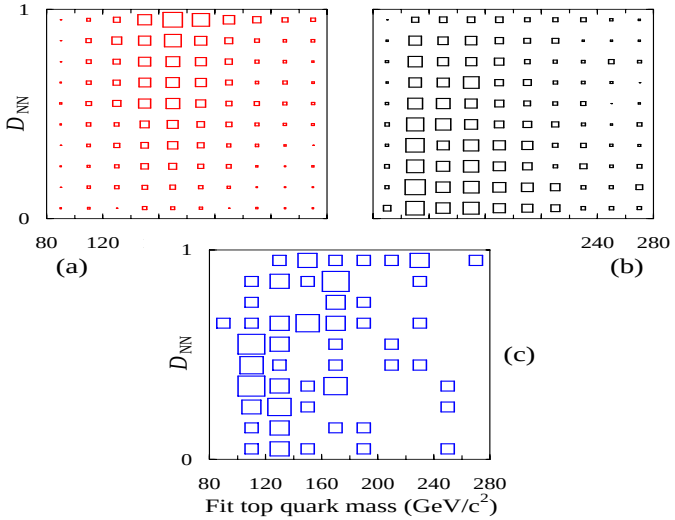

FIG. 14. (DØ) Events per bin ($\propto$ areas of boxes) vs. $\mathcal{D}_{\mathcal{NN}}$ (ordinate) and m_{fit} (abscissa) for (a) expected 172 GeV/c^2 top signal, (b) expected background, and (c) data.

around unity to minimize the average correlation of L with m_{fit}. For each event, the discriminant $\mathcal{D}_{LB}$ is computed as $\frac{L}{1+L}$. For the 2D fit, the samples are divided into signal-rich and background-rich bins; an event falls into signal-rich bin if it has a b-tag or if $\mathcal{D}_{LB} > 0.43$ and $(H_T - E_T^{jet1}) > 90$ GeV.

The NN method naturally takes into account all correlations between the variables used. A three layer feed-forward NN with four input nodes, five hidden nodes and one output node is trained on samples of top (m_t = 170 GeV/c^2) signal MC and background. The NN is trained using the back-propogation algorithm and assigining the output to unity for the signal and zero for the background. For a given event, the network output $\mathcal{D}_{NN}$ directly approximates the ratio $\frac{s(x)}{s(x)+b(x)}$. Fig. 13 shows that $\mathcal{D}_{LB}$ and $\mathcal{D}_{NN}$ are distributed as predicted and provide comparable discrimination. The correlations between $\mathcal{D}_{NN}$ and m_{fit} is displayed for signal, background and data in Fig. 14. Signal peaks at high values of $\mathcal{D}_{NN}$ and at the generated m_t=172 GeV/c^2, whereas the background peaks at lower values of m_{fit} and $\mathcal{D}_{NN}$. Data seems to be a mixture of the two.

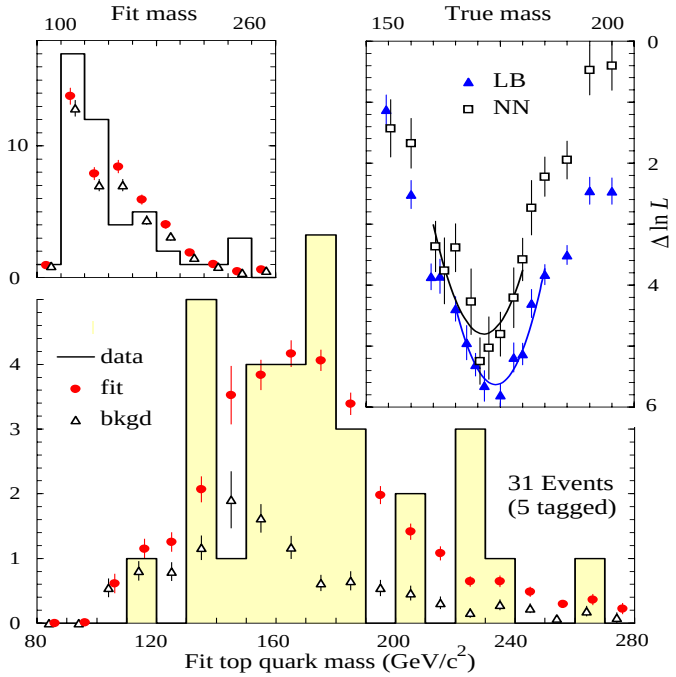

FIG. 15. (DØ) Events/bin *vs.* m_{fit} for (a) background-rich sample and (b) signal-rich sample. The relative $-\ell n\ L$ from the NN and LB fitting methods are shown in (c). The symbols are explained in the legends.

The analyses proceed by binning $(\mathcal{D}_{LB/NN}, m_{fit})$ space into 40 (200) bins in LB (NN) methods and maximizing the likelihood $\mathcal{L}(m_t, n_s, n_b)$ for each m_t, assuming Poisson statistics for each bin and using a Bayesian method [16]; n_s, n_b are the expected number of signal and background events in the data, respectively. Fig. 15 shows the results of the fit and the negative log likelihood, as a function of the top quark mass. This yields $m_t = 174.0 \pm 5.6(stat)$ GeV/c^2 for the LB method and $m_t = 171.3 \pm 6.0(stat)$ GeV/c^2 for the NN method. The total systematic error is estimated to be 5.5 GeV/c^2 (the estimate was 6.2 GeV/c^2 at the time of the conference) for both methods, of which 4.0 GeV/c^2 comes from jet-energy scale and 3.1 GeV/c^2 from various event generator systematics. Combining the LB and NN results, taking into account (88 ± 4) % correlation between them, yields $m_t = 173.3 \pm 5.6(stat) \pm 5.5(sys)$ GeV/c^2.

5.2 CDF Lepton+jets Mass Analysis

Events are selected with the same cuts as in the cross section analysis except for requiring a fourth jet with E_T >15 GeV and $|\eta|$ <2 in the absence of b-tags and, E_T >8 GeV and $|\eta|$ <2.4 in the presence of b-tags.

A constrained 2C kinematic fit for each event yields a fitted mass m_{rec} and a χ^2. After the standard corrections, the energies of the four leading jets are further corrected to the type of parton each is assigned to: a light quark, a hadronically decaying b-quark or a semileptonically decaying b-quark. This parton-specific correction is derived from a study of $t\bar{t}$ events generated with the HERWIG MC. The fit with best χ^2, if $\chi^2 < 10$, is chosen. From the initial sample of 83 events that are fit, 76 events remain after the χ^2 cut.

A maximum likelihood method is used to extract the top mass from the final sample. To make optimal use of all the available information, the sample is partitioned into four non-overlapping sub-samples: (1) events with a single SVX tag, (2)events with two SVX tags, (3)events with an SLT tag but no SVX tag, and (4)events with no tag (untagged).

The global likelihood function is written as a product of three likelihoods: $\mathcal{L} = \mathcal{L}_{shape} \times \mathcal{L}_b \times \mathcal{L}_p$, where $\mathcal{L}_{shape}$ represents the joint probability density for a sample of N reconstructed masses m_i drawn from a population with a background fraction x_b and given by,

$$\mathcal{L}_{shape} = \prod_{i=1}^{N} [(1 - x_b) f_s(m_i|m_t) + x_b f_b(m_i)].$$

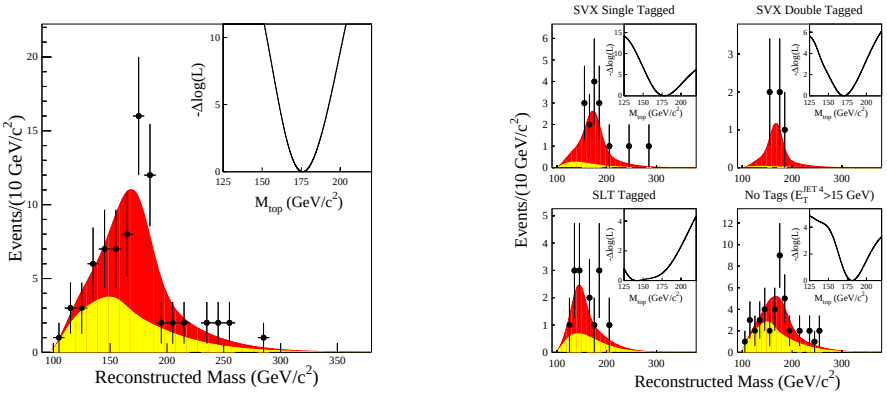

FIG. 16. (CDF) Fitted mass distributions of the combined sample (left) and for the four sub-samples (right). The data are shown as points with errors, the result of the signal+background fit by dark shaded area and the background by the lightly shaded area. The insets show the negative $-\ell n\mathcal{L}$ as a funtion of true top quark mass.

The quantity $f_s(m_i|m_t)$ is the probability to reconstruct a mass m_i for a $t\bar{t}$ event if the true top mass is m_t, and is parametrized as a smooth function of m_i and m_t. The shape of $f_b(m_i)$ is obtained by fitting a smooth function to a mass distribution generated with the VECBOS W+jets MC. The background fraction x_b and the background likelihood function $\mathcal{L}_b$ are generated from a procedure that estimates the unknown numbers of $t\bar{t}$ and W+jets events in the combined sample, by maximizing a multinomial likelihood that constrains the predicted subsample sizes to the observed ones. The independent background measurement corrects the efficiencies from the cross section analysis to include additional cuts used in the mass analysis and predicts the number of events in each mass subsample. The third likelihood $\mathcal{L}_p$ allows the parametrizations of f_s and f_b to vary within the uncertainties allowed by the finite statistics of the signal and background MC samples.

The fitted mass distribution of all 76 events and the combined fit are shown in Fig. 16. The inset shows a quadratic fit to the relative $-\ell n\mathcal{L}$ values as a function of m_t. The combined fit yields m_t=175.9±4.8 GeV/c^2. MC studies yield an 11% probability for obtaining a statistical uncertainty of 4.8 GeV/c^2 or smaller for ensembles of the current sample size. The

Subsample	N_{obs}	x_b (%)	Measured m_t (GeV/c^2)
SVX double tag	5	5±3	170.1±9.3
SVX single tag	15	13±5	178.0±7.9
SLT tag (no SVX)	14	40±9	142.0^{+33}_{-14}
No tag	42	56±15	181.0±9.0

TABLE IV. Subsamples used in the CDF mass measurements in the *lepton+jets* channel, the number of observed events N_{obs}, the expected background fraction x_b and the measured top quark mass m_t in each case. Uncertainties in the measured m_t are statistical only.

fitted mass distribution in each of the four sub-samples is compared to the results of the fit in Fig. 16. The results are shown in Table IV. The dominant source of systematic error in m_t is the uncertainty in the jet energy measurement which is $\sim$ 4.4 GeV/c^2, for the combined fit. The total systematic uncertainty is estimated to be 4.9 GeV/c^2.

5.3 DØ Dilepton Mass Analysis

DØ has five *dilepton* candidate events (3 $e\mu$, 1 ee and 1 $\mu\mu$) after the initial selection criteria used in the cross section measurement. Another ee event is picked up by relaxing the track requirement on one of the electrons when a b-tag is present. These six events are used to measure the top quark mass. The expected backgrounds are 0.21±0.16, 0.47±0.09 and 0.73±0.25 events in the $e\mu$, ee and $\mu\mu$ channels, respectively.

Two methods are used to solve the $t\bar{t}$ decay by assuming values for m_t and η for each of the two undetected neutrinos. There are up to four possible solutions for the neutrino momenta; each solution is weighted by its likelihood for occurence in a $t\bar{t}$ event for the assumed m_t.

In the *matrix element weighting* ($\mathcal{M}$WT) method, a modified version of the procedure first suggested by Dalitz and Goldstein [17], a weight proportional to the product of the structure functions for top and antitop and probability densities of the lepton energies in the rest frame of the decaying top, is assigned. In the neutrino weighting (νWT) method, the expected phase space of neutrino pseudorapidity in $t\bar{t}$ events (at a given m_t) is spanned in steps of equal fraction. For each pair of assumed neutrino η, a weight is asigned to each of the solutions based on the extent to which the

p_T^ν's from the solution agree with the measured $\not\!\!E_T$ in the event. The weight at all η values are summed to give $W_o(m_t)$. Detector resolutions are taken into account by fluctuating the measured objects by appropriate resolutions 100 (5000) times for MC (data) events. For each event, the weights are summed over the ambiguous neutrino solutions as well as the two possible pairs of jets with leptons. If the event has more than two jets (due to ISR or FSR), a weighted sum over all possible combinations of the three leading jets is taken.

The final normalized distributions of $W(m_t)$ for the six candidate events are shown in Fig. 17. A maximum likelihood fit is performed to the expectations from signal and background. The signal is modeled using HERWIG, the backgrounds are modeled by ISAJET and PYTHIA and DØ data. To make use of the information contained in the shape of the weight distribution as a function of m_t, the integrated weights $\bar{w}_i$ in four of the five 40 GeV/c^2 bins in m_t are used in the maximum likelihood fit. The likelihood $\mathcal{L}(m_t, n_s, n_b)$ is writen as

$$\mathcal{L} = g(n_s)g(n_s + n_b) \times \frac{n_s f_s(\bar{w}_i, m_t) + n_b f_b(\bar{w}_i)}{n_s + n_b}$$

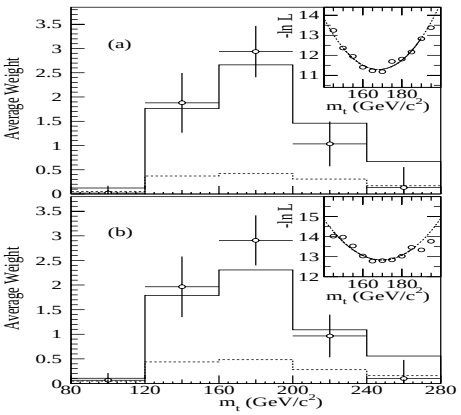

FIG. 17. The distributions of weights from the two DØ dilepton mass analyses. The insets show the negative log-likelihood as a funtion of true top quark mass.

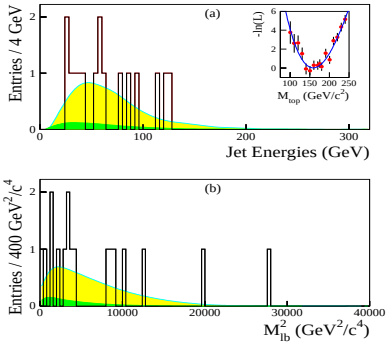

FIG. 18. The distributions of the b-jet energies and of M_{lb}^2 from the CDF analyses. The inset shows the negative log-likelihood as a funtion of true top quark mass, for the first method.

where n_s and n_b are the fitted signal and background levels, $g(n_b)$ is a Gaussian constraint on n_b, $p(n_s + n_b)$ is a Poisson constraint on $(n_s + n_b)$ constrained to the sample size N, f_s and f_b are the four dimensional probability densities of signal and background. The $f(\bar{w})$'s are estimated using a multivariate probability density method [18]. The maximum likelihood estimate of m_t and its error are determined by a quadratic fit to $-ln\mathcal{L}$ using nine points about the minimum. The insets in Fig. 17 show the $ln\mathcal{L}$ distributions from which top quark mass $m_t = 168.1 \pm 12.4$ GeV/c^2 ($\mathcal{M}WT$) and $m_t = 169.9 \pm 14.8$ GeV/c^2 (νWT) are extracted. The total systematic uncertainty in the measured m_t due to jet energy scale, signal and background modeling, likelihood fit and multiple interactions is estimated to be 3.6 GeV/c^2.

Combining the results from $\mathcal{M}WT$ and νWT analyses, taking into account the 77% correlation between them, yields $m_t = 168.4 \pm 12.3 \pm 3.6(sys)$ GeV/c^2. When combined with DØ's mass measurement from *lepton+jets* channel one obtains, $m_t = 172.1 \pm 5.2(stat) \pm 4.9(sys)$ GeV/c^2.

5.4 CDF Dilepton Mass Analysis

The CDF collaboration has also measured the top quark mass from *dilepton* events using two different techniques. Using event selection cuts as in the cross section analysis and H_T >170 GeV, 6 $e\mu$, 1 ee and 1 $\mu\mu$ events are selected. The first method compares E_T of the two b-quark jets from $t\bar{t}$ decay is directly related to the top quark mass. This method yields a mass of $159^{+24}_{-22}(stat) \pm 17(sys)$ GeV/c^2. The second method uses the relation between the invariant mass M_{lb} of the charged lepton and the b-quark and the top mass, $m_t^2 = \langle M_{lb}^2 \rangle + \sqrt{M_W^4 + 4M_W^2 \langle M_{lb}^2 \rangle + \langle M_{lb}^2 \rangle^2}$. This analysis yields $m_t = 163 \pm 20(stat) \pm 9(sys)$GeV/$c^2$. Fig. 18 shows the distribution of the b-jet energies and of M_{lb}^2.

5.5 CDF All-Jets Top Mass Analysis

CDF uses events selected with the first approach of the cross section analysis in the *all-jets* channel. Further requiring 5< N_{Jets} <10 and $\sum E_T^{jet}$ >200 GeV, 136 events with at least 1 SVX b-tag are observed.

The reconstructed top mass distribution and the likelihood fit are displayed in Fig. 19. The background distribution is calculated by normalizing the spectrum of untagged sample of 1121 events to 108±9 events, estimated

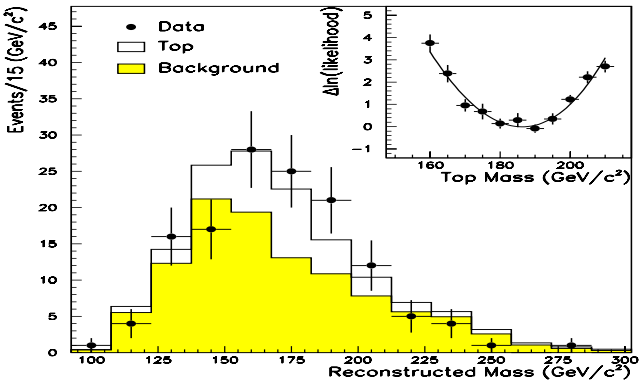

FIG. 19. Maximum likelihood fit to the reconstructed top mass from CDF *all-jets* analysis.

using the tag probability. A maximum likelihood fit performed with HERWIG MC events for $t\bar{t}$ sample and the untagged events to model the background, yields m_t =186 $\pm$ 10 (stat) GeV/c^2. The total systematic uncertainty is estimated to be $\pm$6.2% or 12 GeV/c^2.

6. Other Studies

Both CDF and DØ collaborations have studied kinematic properties such as the p_T and rapidity of the $t\bar{t}$ system, rapidity difference between t and $\bar{t}$, invariant mass $m_{t\bar{t}}$, using selected candidate events. All are found to be in agreement with SM expectations within present statistical uncertainties. Searches for charged Higgs in top decays have also been carried out and limits have been set [19,20]. CDF has also set limits on some rare decays: $BR(t \to q\gamma) < 2.9\%$ (95% C.L.) and $BR(t \to qZ) < 44\%$ (95% C.L.). By measuring $B = BR(t \to Wb)/BR(t \to Wq) = 1.23^{+0.37}_{-0.31}$ ($B > 0.61$ at 95% C.L.), CDF sets a limit on the CKM matrix element V_{tb} >0.050 at the 95% C.L.

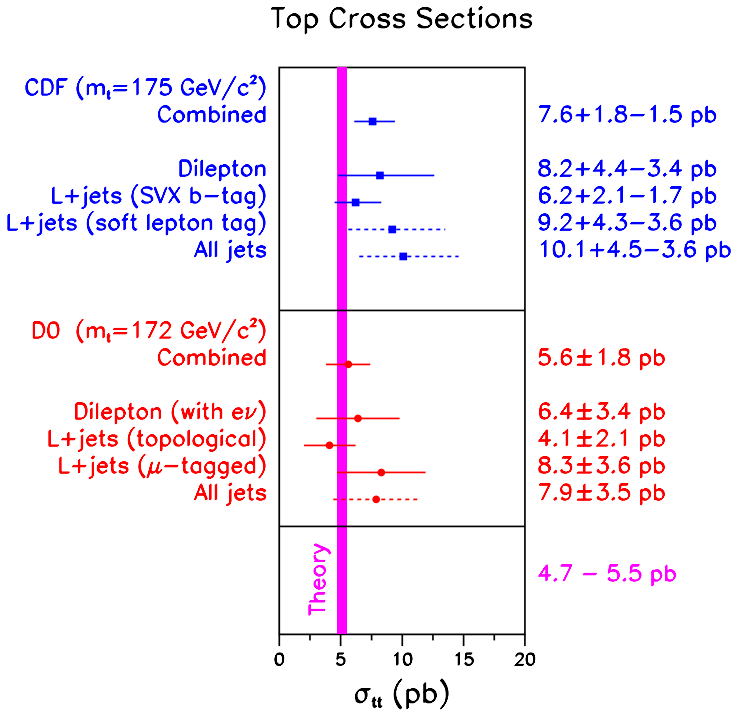

FIG. 20. Summary of $t\bar{t}$ production cross section measurements.

7. Summary and Future Prospects

We have reviewed the analyses of the $p\overline{p}$ data ($\sqrt{s}$=1.8 TeV), carried out by CDF and DØ to select $t\bar{t}$ events and study the physics of the top quark. The $t\bar{t}$ production cross section measurements in various channels are summarized in Fig. 20. The combined measurements are $\sigma_{t\bar{t}} = 7.6^{+1.8}_{-1.5}$ pb (at m_t = 175 GeV/c^2) by CDF and $\sigma_{t\bar{t}}$ = 5.6±1.8 pb (at m_t=172 GeV/c^2) by DØ. The top quark mass measurements are summarized in Fig. 21. The world average direct measurement (combining CDF and DØ results) in the *lepton+jets* channel is m_t=174.8±5.5 GeV/c^2(unofficial). Though limited by statistics, a number of other studies have been carried out and the results are found to be consistent with SM expectations.

The upgraded detectors will resume taking data (Run II) with the Tevatron augmented by the "Main Injector", beginning in the year 2000. The integrated luminosity per experiment is expected to be 2 fb^{-1}. Precision measurement of the top quark mass and $t\bar{t}$ production cross section, ob-

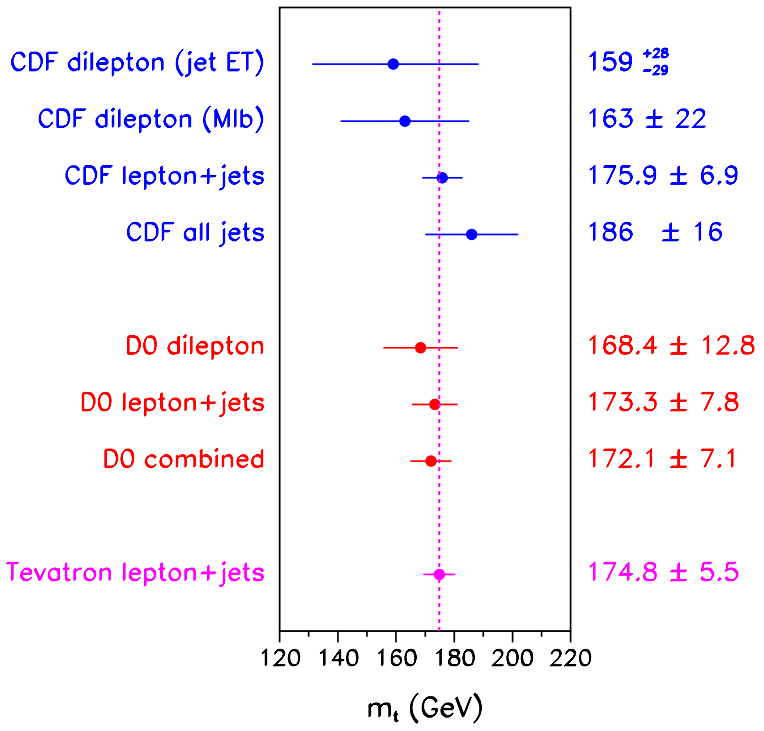

FIG. 21. Summary of top quark mass measurements.

servation and study of single top production and, search for hints of new physics will be pursued using the $\sim 40-50$ times larger top event samples.

Acknowledgements

We thank the Fermilab Accelerator, Computing, and Research Divisions, and the support staffs at the collaborating institutions for their contributions to the success of this work. This work is supported in part by the U.S. Department of Energy.

REFERENCES

[1] F. Abe *et al.*, (CDF Collaboration), Phys. Rev. Lett. **74**, 2626 (1995).

[2] S. Abachi *et al.*, (DØ Collaboration), Phys. Rev. Lett. **74**, 2632 (1995).

[3] F. Abe *et al.*, (CDF Collaboration), Nucl. Instrum. Methods **A271**, 387(1988).

[4] S. Abachi *et al.*, (DØ Collaboration), Nucl. Instrum. Methods **A338**, 185(1994).

[5] F. Abe *et al.*,(CDF Collaboration), Phys. Rev. **D50**, 2966 (1994).

[6] S. Abachi *et al.*, (DØ Collaboration), Phys. Rev. **D52**, 4877 (1995).

[7] A. P. Heinson, A. S. Belyaev and E. E. Boos, Phys. Rev. **D56**, 3114 (1997).

[8] E. Berger and H. Contopanagos, Phys. Rev. **D54**, 3085 (1996); S. Catani *et al.*,*Phys. Lett.* B**378**, 329 (1996); E. Laenen, J. Smith and W. L. van Neerven, *Phys. Lett.* B**321**, 254 (1994).

[9] S. Abachi *et al.*, (DØ Collaboration), Phys. Rev. Lett. **79**, 1203 (1997).

[10] F. Abe *et al.*, (CDF Collaboration), Phys. Rev. Lett. **79**, 1992 (1997); Phys. Rev. Lett. **79**, 3585 (1997); Phys. Rev. Lett. **80** (1998).

[11] G. Marcheseini and B.R. webber, Nucl. Phys. B **310**, 461 (1988); G. Marcheseini *et al.* Comput. Phys. Commun. **67**, 465 (1992).

[12] B. Abbott *et al.*, (DØ Collaboration), Phys. Rev. Lett. **79**, 1197 (1997); A detailed paper submitted to *Phys. Rev.* D; Phys. Rev. Lett. **80** (1998).

[13] N. Amos *et al.*, Proceedings of the Computing in High Energy Physics Conference, Rio de Janeiro, Brazil, (1995).

[14] N. Amos (for the DØ Collaboration), Proceedings of the Workshop on Hadron Collider Physics, Stony Brook, NY, USA (1997).

[15] P.C. Bhat (for the DØ Collaboration), Proceedings of the 10th Topical Workshop on Proton-Antiproton Collider Physics, Fermilab, Batavia, USA, (1995), p. 308 (FERMILAB-Conf-95/211-E); P. C. Bhat (for DØ) in the Proceedings of the 8th meeting of DPF, Albuquerque, NM, USA (1994), p. 705.

[16] P. C. Bhat, H. B. Prosper and S. Snyder, *Phys. Lett.* B**407**, 73 (1997).

[17] R.H. Dalitz and G.R. Goldstein, Phys. Rev. D **45** , 1531 (1992) and Phys. Lett. B **287**, 225 (1992); E. Varnes, Ph.D. thesis, University of California at Berkeley, 1997 (unpublished).

[18] L. Holmstrom, R. Sain and H. .E. Miettinen, Comp. Phys. Comm. **88**, 195 (1995); Also see ref. [15].

[19] F. Abe *et al.*, (CDF Collaboration), Phys. Rev. Lett. **79**, 357 (1997).

[20] M. Strovink (for the DØ Collaboration), Proceedings of International Europhysics Conference on High Energy Physics, Jerusalem, Israel (1997), Fermilab-Conf-97/386-E.